Heliyon 6 (2020) e04331

Contents lists available at ScienceDirect

Heliyon

journal homepage: www.cell.com/heliyon

Research article

Identification and sub-cellular localization of a NAD transporter in *Leishmania braziliensis* (*Lb*NDT1)

David S. Morales Herrera [a], Luis E. Contreras Rodríguez [a], Claudia C. Rubiano Castellanos [a], Maria H. Ramírez Hernández [a,b,*]

[a] Laboratorio de Investigaciones Básicas en Bioquímica, Facultad de Ciencias, Universidad Nacional de Colombia, Bogotá, 111321, Colombia
[b] Departamento de Biología, Facultad de Ciencias, Universidad Nacional de Colombia, Bogotá, 111321, Colombia

ARTICLE INFO

Keywords:
Cell biology
Bioinformatics
Biochemistry
Molecular biology
Biomolecules
NAD transport
Energetic metabolism
Leishmania braziliensis
*Lb*NDT1

ABSTRACT

Nicotinamide adenine dinucleotide (NAD) is one of the central molecules involved in energy homeostasis, cellular signaling and antioxidative defense systems. Consequently, its biosynthetic pathways and transport systems are of vital importance. The nicotinamide/nicotinate mononucleotide adenylyltransferase (NMNAT), a key enzyme in the biosynthesis of NAD, is distributed in all domains of life and exhibits various isoforms in free-living organisms in contrast with intracellular parasites, which displays a single enzyme. In *Leishmania braziliensis* a unique cytosolic NMNAT has been reported to date and the mechanisms through which adequate levels of NAD are maintained among the different sub-cellular compartments of this parasite are unknown. Experimental evidences have related the transport of NAD to the Nucleotide Transporters (NTTs) family, whose members are located in the cytoplasmic membrane of parasitic life organisms. Additionally, the Mitochondrial Carrier Family (MCF), a group of proteins located in the membrane of internal organelles such as the mitochondria of free life organisms, has been implicated in NAD transport. Applying bioinformatics tools, the main characteristics of the MCF were found in a transporter candidate that we have designated as Nicotinamide Adenine Dinucleotide Transporter 1 of *L. braziliensis* (*Lb*NDT1). The expression of *Lb*NDT1 was tested both in axenic amastigotes and promastigotes of *L. braziliensis*, through immunodetection using polyclonal avian antibodies produced in this study. N-glycosylation of *Lb*NDT1 was observed in both stages. Additionally, a possible partial mitochondrial distribution for *Lb*NDT1 in amastigotes and a possible glycosomal location in promastigotes are proposed. Finally, the capability of *Lb*NDT1 to transport NAD was confirmed by complementation assays in *Saccharomyces cerevisiae*. Our results demonstrate the existence of *Lb*NDT1 in *L. braziliensis* becoming the first NAD transporter identified in protozoan parasites to date.

1. Introduction

Nicotinamide adenine dinucleotide (NAD) exerts central metabolic and regulatory functions, as it participates as coenzyme and substrate in redox and cell signaling reactions, respectively. Sirtuins, glycohydrolases, mono and poly ADP ribosyl transferases (ARTs, PARPs), utilize NAD as substrate to regulate vital processes such as DNA repair, cell death, circadian rhythm and genetic expression, among many others (Nikiforov et al., 2015). Therefore, the biosynthesis and transport of NAD are crucial to maintain its optimal levels in the cell.

Two pathways carry out NAD biosynthesis, the *de novo* and salvage pathways, which use as precursors amino acids as tryptophan and subproducts of NAD metabolism as nicotinamide, respectively. Both pathways converge in the step catalyzed by the nicotinamide/nicotinate mononucleotide adenylyltransferase (NMNAT) enzyme (VanLiden et al., 2015). This enzyme has been identified in extracellular organisms as *Giardia duodenalis* that possesses 2 isozymes (*Gd*NMNAT1-2) (Forero-Baena et al., 2015) and *Saccharomyces cerevisiae* which has 3 isozymes (*Sc*NMNAT1-3) (Emanuelli et al., 1999, 2002; Kato and Lin, 2014); in *Homo sapiens* 3 isozymes (*Hs*NMNAT1-3) located in the nucleus, the Golgi apparatus and the mitochondria have been reported (Berger et al., 2005). Interestingly, a unique isoenzyme has been identified in intracellular parasites such as *Leishmania braziliensis* (*Lb*NMNAT) (Contreras et al., 2015), *Tripanosoma cruzi* (*Tc*NMNAT) (Niño et al., 2015) and *Plasmodium falciparum* (*Pf*NMNAT) located in the cytoplasm (O'Hara et al., 2014). In these pathogens, the NAD transport mechanisms remain unanalyzed.

* Corresponding author.
E-mail address: mhramirezh@unal.edu.co (M.H. Ramírez Hernández).

https://doi.org/10.1016/j.heliyon.2020.e04331
Received 18 December 2019; Received in revised form 18 April 2020; Accepted 24 June 2020

The transport of nucleotides depends on membrane proteins, which belong to two families: the Nucleotide Transporters (NTTs) and the Mitochondrial Carrier Family (MCF). The NTTs members are located in the cytoplasmic membrane and possess 12 trans-membrane regions, while the MCF members are located in the membrane of internal organelles and exhibit 6 trans-membrane regions. The proteins of both families have the capacity to translocate NAD and ADP, displaying a preference for the oxidized form of NAD (NAD+) (Palmieri et al., 2009). Carriers of the NTT family have been identified in intracellular organisms as the bacteria *Protochlamydia amoebophila* which has 5 members (*Pam*NTT1-5) from which *Pam*NTT4 has high affinity for NAD+ (Haferkamp et al., 2006) and *Chlamydia trachomatis* which has 2 members (*Ct*NTT1-2) from which *Ct*NTT1 has the capacity to translocate ATP or NAD+ (Fisher et al., 2013; Haferkamp et al., 2004b). Additionally, NAD+ transporters belonging to the MCF have been described in free-living organisms: *S. cerevisiae* with 2 proteins (ScNdt1p-2p), located in the internal membrane of the mitochondria (Todisco et al., 2006); *Arabidopsis thaliana* with two proteins (*At*NDT1-2), in the internal membrane of chloroplast and mitochondria, respectively (Palmieri et al., 2009), and *H. sapiens* with 3 proteins (SLC25A17-33-36) one in the peroxisome membrane and the other two in the internal membrane of the mitochondria and with affinity toward pyrimidine nucleotides (Agrimi et al., 2012; Di Noia et al., 2014).

L. braziliensis is one of the etiological agents of Leishmaniasis, a parasitic disease that affects about 20 million people worldwide according with the OPS and OMS. The current treatment includes chemotherapy with pentavalent antimony salts (Sb^{+5}), amphotericin B and miltefosine; nevertheless, these treatments generate serious side effects in the host and resistant strains have been identified. As such, it is fundamental to identify new drugs and potential therapeutic targets (Sundar and Singh, 2018). For this reason, the study of the transport of NAD in this pathogenic agent constitutes a contribution in the identification of new possible therapeutic targets.

In this study the existence of NAD transporters in *L. braziliensis* is proposed; as such, a candidate membrane protein (*Lb*NDT1) was identified through bioinformatics tools, its functional characterization was completed in terms of protein expression, posttranslational modification and subcellular localization in axenic amastigotes and promastigotes. The functional evaluation of *Lb*NDT1 was carried out by complementation assays in *S. cerevisiae*, verifying the capacity of the proposed candidate to partially restore the phenotype of a mutant strain.

2. Materials and methods

2.1. Bioinformatic approach

The selection of the candidate for the NAD transporter in *L. braziliensis* (*Lb*NDT1, XM_001568380.1 on NCBI) was carried out with PSI-BLAST on the NCBI server using the genome of *L. braziliensis* (M2904 MHOM/BR/75M2904) and a consensus sequence obtain from a multiple sequence alignment of experimentally characterized NAD transporters that was built by progressive alignment using the CLC Sequence Viewer 6.8.1 software (https://www.qiagenbioinformatics.com). The domains and motifs on the selected sequence were evaluated with INTERPRO (Mitchell et al., 2019), MotifFinder NCBI-CDD, CCTOP (Dobson et al., 2015) and PHYRE2 (Kelley et al., 2015) servers. Additionally, a predictive model was obtained of tertiary structure with ROBETTA server (Pettersen et al., 2004), which was validated by Ramachandran plot (Lovell et al., 2003). The structures were visualized and compared with UCSF Chimera software (1.8.1 version) (Pettersen et al., 2004). Finally, the possible glycosylation on the proposed candidate was predicted by GlycoEP (Chauhan et al., 2013), NetOGlyc-4.0 (Steentoft et al., 2013) and NetNGlyc-1.0 (Blom et al., 2004) servers.

2.2. Experimental approach

2.2.1. L. braziliensis culture and extraction fo genoic DNA

Promastigotes of *L. braziliensis*, MHOM/BR/75M2904 strain, were cultivated in Schneider's Medium (Sigma), supplemented with fetal bovine serum (FBS) at 10 %(v/v) (Gibco) at 27 °C. The parasites were collected by centrifugation at 6,000 g for 10 min and afterward resuspended in 200 μL of lysis buffer (10 mM Tris-HCl pH 8.5, 5 mM EDTA, 0.5 %(w/v) SDS, 200 mM NaCl and 100 μg/mL proteinase K) and then incubated for 30 min at 65 °C (Lagos M et al., 2007). Finally, the total DNA of the parasite was obtained via precipitation with 2 volumes of absolute ethanol. On the other hand, the axenic amastigotes were gotten from the differentiation of promastigotes induced by growth in the medium RPMI-1640 (Sigma) pH 6.4 supplemented with fetal bovine serum (SFB) at 10 %(v/v) at 37 °C in 25 cm^2 (T25) flask with no agitation.

2.2.2. Cloning of Lbndt1 of L. braziliensis

From 200 ng of genomic DNA of promastigotes of *L. braziliensis* the amplicon of *Lb*ndt1 (1.089 pb) was obtained by PCR (Gibbs, 1990) with Taq DNA polymerase and the primers: forward with the recognition site for BamHI 5′-**GGATCC**ATGACGCAGTCTTTC-3′ and the reverse with the recognition site for EcoRI 5′-**GAATTC**CTACTGGAACTGAGGC-3′. The conditions of reaction were as follows: 1 U of Taq polymerase in reaction buffer (50 mM KCl, 10 mM Tris-HCl pH 8.3 and 0,1 %(v/v) Tritón, 2.0 mM $MgCl_2$, dNTPs (dATP, dGTP, dCTP, dTTP), forward and reverse primers at 0.2 μM in a final volume of 15 μL. The thermal cycle was an initial denaturalization at 94 °C for 10 min, followed by 20 cycles of amplification (denaturalization at 94 °C for 30 s, *annealing* at 57 °C for 1 min and elongation at 72 °C for 1 min); finally a cycle of elongation was carried out at 72 °C for 10 min (Veriti Thermo Cycle, Applied Biosystems). The amplicon was sub-cloned in the pGEM-T Easy (Promega) vector, the product was digested by enzymatic restriction and cloned into pYES2 (Invitrogen) vector. As a positive control for the assays of complementation the amplicon of *At*NDT2 of 1.093 pb (NM_102349.4 in NCBI) was obtained from 100 ng of cDNA of *A. thaliana* (donated by Doctor Camilo López, Biology department, Universidad Nacional de Colombia, Bogotá campus) as a template with Taq DNA polymerase and the primers: forward with recognition site for BamHI 5′-**GGATCC**ATGATTGAACATGGG-3′ and reverse with recognition site for EcoRI 5′-**GAATTC**TTATTTGCTTCCAAGAGG-3′; the *annealing* temperature was 60 °C. Both amplification and cloning of *At*NDT2 were carried out under the same conditions used for *Lb*NDT1. The corresponding inserts were verified by sequencing. The results were evaluated by electrophoresis in agarose gel at 0.8 %(w/v) dyed with ethidium bromide (0.05 %(v/v) and documented in the image analyzer Imager® Gel DocTMXR, with Quantity One Basic 4.6.3 de BIORAD™ (software).

2.2.3. Complementation assays in S. cerevisiae

The culture of *S. cerevisiae* BY4741 ΔNDT1 (MATa; ura3Δ0; leu2Δ0; his3Δ1; met15Δ0, YIL006w::kanMX4, Y01398 in EUROSARnF) strain and INVSc1 (MATa/α; his3Δ1; leu2; trp1-289; ura3-52, Invitrogen) wild strain were kept in the liquid YPD medium (1 %(w/v) extract of yeast, 2 %(w/v) peptone and 2 %(w/v) glucose, Sigma) at 30 °C with constant agitation. The solid YPD medium, was supplemented with bacteriological agar at 2 %(w/v) (Todisco et al., 2006). For the obtention of the transfectants, electroporation cells of 0.4 cm (Bio-Rad) were utilized. To 50 ng of the plasmids *Lb*NDT1/pYES2, *At*NDT2/pYES2 and empty pYES2, 80 μL of the electrocompetent cells were added, then gently shaken and incubated for 10 min; after that, a unique pulse of 5 ms of 2.5 kV was applied (Gene Pulser XcellTM Electroporation System, Bio-Rad). Later, the cells were recovered with 1 mL of 1 M sterile sorbitol for 15 min at room temperature and finally the selection of the transfectants were carried out

on Minimal Synthetic Ura$^-$ plates (MS-Agar) and incubated at 30 °C for 36 h.

The growth of the transfectants obtained was evaluated in liquid and solid mediums MS Ura$^-$. In both cases pre-inoculums in medium MS Ura$^-$ supplemented with glucose at 2 %(w/v) were incubated for 14 h at 30 °C under constant agitation; next, aliquots of each inoculum were taken to obtain a final OD_{600} of 0.2 in 15 mL of medium. Each aliquot was pellet at 7,168 g for 10 min at 4 °C; then the supernatants were thrown up and the cellular pellets were re-suspended in 15 mL of de induction medium MS Ura$^-$ supplemented with fermentable carbon source (raffinose) or not fermentable (ethanol) at 2 % (w/v) and 0.1 % (w/v) galactose. For the evaluation of the growth in the liquid medium the cultures were incubated at 30 °C under constant agitation and readings of OD_{600} were carried out every 24 h for 4 days. For the evaluation in solid medium three 1/10 serial dilutions of each inoculum (OD_{600} initial of 0.2) were carried out with the induction medium, and 10 μL of each one were plated on MMS Ura$^-$ plates supplemented with 2 % (w/v) ethanol and 0.1 %(w/v) galactose + 2 %(w/v) Agar and incubated at 30 °C. The growth was documented every 24 h for 4 days with the image analyzer Image® Gel DocTMXR and software Quantity One Basic 4.6.3 de BIO-RAD™ (Palmieri et al., 2009; van Roermund et al., 2016; Todisco et al., 2006).

2.2.4. Immunodetection of Trx-LbNDT1 by SDS-PAGE and western blot

The samples were evaluated by SDS-PAGE (Roy and Kumar, 2014) at 12 %(w/v) and dyed with Coomassie R-250 blue or electro-transferred to a nitrocellulose membrane (Millipore) by application of 200 mA for 2 h in transfer buffer (10 mM Tris/HCl pH 8.0, 0.2 M glycine, 10 %(v/v) methanol). The membrane was blocked all night with 5 %(w/v) skimmed milk in TBST (20 mM Tris-HCl pH 7.5, 150 mM NaCl, 0.1 %(v/v) Tween20. The immunodetection of the recombinant protein was performed by western blot (Yang and Mahmood, 2012) using the monoclonal primary antibody anti-thioredoxin (1:6.000), the secondary antibody anti-mouse IgG conjugated to biotin (Sigma, B7264) (1:10.000) in TBST and Streptavidin conjugated alkaline phosphatase (Promega) (1:5.000) in TBST. NBT and BCIP (Promega) were used as substrates.

2.2.5. Production of avian polyclonal antibodies α-LbNDT1

From 200 ng of genomic DNA (from promastigotes of *L. braziliensis* MHOM/BR/75M2904 strain) the amplicon of *Lb*ndt1 (1.089 pb) was obtained by PCR with *Pfu* DNA polymerase and the primers forward 5′-**CACC**ATGACGCAGTCTTTCTCATCA-3′ and reverse 5′- CTACTGGAACTGAGG CTGTCCCACA-3′. The reaction conditions were the following: 1 U of *Pfu* polymerase in reaction buffer (20 mM Tris-HCl pH 8.8, 10 mM $(NH_4)_2SO_4$, 10 mM KCl, 0.1 %(v/v) Triton X-100, 0.1 mg/mL BSA), 2.5 mM $MgSO_4$, 0.2 mM dNTPs (dATP, dGTP, dCTP, dTTP), forward and reverse primers at 0.2 μM in a final volume of 25 μL. The thermic cycle was carried out under previously-described conditions with an *annealing* temperature of 57 °C. The corresponding insert was cloned in the vector pBAD202/d-TOPO (Invitrogen) which provides a thioredoxin tag at the N-Terminal of the recombinant protein. Finally, the recombinant vector was verified by sequencing.

E. coli BL21 (DE3) chemically competent cells (Invitrogen) were transformed by heat shock with the recombinant plasmid obtained and the resulting product was inoculated in *LB* liquid medium supplemented with 100 μg/mL of Kanamycin, up to OD_{600nm} of 0.6. The expression of the recombinant protein Trx-*Lb*NDT1 was carried out by the addition of L-Arabinose 0.02 % (w/v) for 4 h at 37 °C (conditions previously standardized). The cells were collected by centrifugation at 4,032 g for 10 min and lysed by sonication in ice bath for 16 min (pulses of 15 s and rest of 45, amplitude of 50%, 130 Watt Ultrasonic Processors) in lysis buffer (50 mM NaH_2PO_4 pH 8.0, 400 mM NaCl, 100 mM KCl, 10% (v/v) glycerol, 0.5% (v/v) Triton X-100, 10 mM imidazole) supplemented with lysozyme (0.5 mg/mL) and protease inhibitor cocktail (1:400) (Sigma P8340: 1 mM AEBSF, 14 μM E64, 15 μM Pepstatin A, 40 μM Bestatin, 20 μM Leupeptin, 0,8 μM Aprotinin).

The separation of the soluble and insoluble protein fractions was done by centrifugation of the lysed cells at 16,128 g for 30 min. The inclusion bodies present in the insoluble fraction were extracted by washes according with the protocol reported previously (Palmer and Wingfield, 2012). The final product was dialyzed for 24 h at 4 °C in 500 mL of 20 mM Tris-HCl and 300 mM NaCl, pH 7.5 buffer, with a buffer change at 12 h. Additionally, the product of dialysis was pellet at 16,128 g for 20 min at 4 °C. The corresponding pellet with partially purified protein was loaded into a preparative gel of 16 × 19 cm at 12 % (w/v); the bands that contained the protein split from the gel by comparing with the pre-stained molecular weight marker (Pre-stained Protein Ladder – Broad molecular weight 10–245 kDa, abcam). Then they were pulverized and the protein was eluted with deionized water at 37 °C under constant agitation. The purification process was followed by SDS-PAGE at 12 %(w/v) and the resultant protein was quantified by densitometry using ImageJ software (Herrera et al., 2019).

The production of the antibodies was carried out with Badcock Brown hens (32 weeks old) by an initial inoculation of 150 μg of purified recombinant protein with Freund's complete adjuvant and three booster injections of the same amount of protein and Freund's incomplete adjuvant (Moreno-González et al., 2013). Finally, the specific antibodies α–*Lb*NDT1 were purified by antigen affinity using the recombinant protein in nitrocellulose membranes from the immunogenic serums collected after each inoculation (Smith and Fisher, 1984).

2.2.6. Immunodetection and immunolocation of LbNDT1 in axenic amastigotes and promastigotes of L. braziliensis

The total protein extracts, soluble and insoluble fraction of axenic amastigotes and promastigotes of *L. braziliensis* (M2904 MHOM/BR/75M2904) were gotten from parasites pelleted by centrifugation at 7,168 g for 10 min at 4 °C, which were washed 3 times with phosphate buffer (PBS) pH 7.4 and then again were pelleted in order to obtain the cellular fraction which, in turn, was re-suspended in 500 μL of lysis buffer (0.1X PBS, Triton X-100 and protease inhibitor cocktail 1:200); then it was incubated at 4 °C for 30 min under constant agitation and pellet at 16,128 g for 5 min at 4 °C. Next, the supernatant (soluble protein fraction) and the pellet (insoluble protein fraction) were separated. From the parasites gathered initially an aliquot was taken and lysed with loading buffer 1X for SDS-PAGE (total extract). After the cellular lysis, the samples were loaded in discontinuous SDS-PAGE gels at 12 %(w/v) and the immunodetection of endogenous *Lb*NDT1 was performed by western blot on nitrocellulose membranes with the IgY's α–*Lb*NDT1 purified (1:100) as primary antibody. For the secondary antibody, biotinylated donkey IgG α-IgY (1:10,000) was used and the revelation system with streptavidin conjugated alkaline phosphatase and a BCIP/NBT substrates (alkaline phosphatase system).

From 1 mL of confluent cultivation of axenic amastigotes or promastigotes of *L. braziliensis*. The parasites obtained by centrifugation at 2,800 g for 5 min at 4 °C were then washed 3 times with PBS by centrifugation. The cell pellet was re-suspended in PBS and approximately 2 × 10^5 cells on glass slides treated with poly-L-lysine were applied. Next, the cells were attached with 4 %(w/v) paraformaldehyde for 1 h at 4 °C. Also, they were incubated with 100 mM glycine for 15 min, permeabilized with acetone for 10 min at 4 °C and blocked with 1 %(w/v) BSA for 1 h. As primary antibody the produced IgY's α-*Lb*NDT1 (1:100 o 1:10 in blocking solution) were used and the secondary anti-IgY conjugated to Alexa Fluor 488 (1:1,000 in blocking solution) (Invitrogen) were then incubated for 1 h (the secondary one in darkness). The nuclei were stained with 1 μg/μL 4′,6-diamidino-2-phenylindole (DAPI) for 5 min. For the mitochondrial staining, axenic amastigotes were incubated in RPMI-1640 medium (Sigma) without SFB at 37 °C for 30 min and the promastigotes in Schneider medium (Sigma) without SFB at 26 °C, simultaneously, with Mitotracker Red CMXRos dye (1 μM) (Invitrogen) (Leprohon et al., 2009). The glass slides were covered with mounting solution (Fluoromont-G, Invitrogen) and the images were observed and

recorded using the Nikon C1 fluorescence microscope Nikon C1 Plus ECLIPSE Ti and were analyzed with the NIS Elements AR software.

3. Results

3.1. *LbNDT1 of L. braziliensis shows typical structural elements of the Mitochondrial Carrier Family (MCF)*

Our bioinformatics exploration in the genome of *L. braziliensis* (MHOM/BR/75/M2904), revealed a NAD transporter candidate (NCBI, XM_001568380.1) with reliable search parameters (sequence identity 21.58%, coverage 88%, E-value 4.0×10^{-9}). The identified 1,089 pb genomic sequence codifies a protein of 362 amino acids residues with a theoretical molecular weight of 39.8 kDa. The candidate was designated as Nicotinamide adenine Dinucleotide Transporter 1 of *L. braziliensis* (*Lb*NDT1). Functional domains analysis of *Lb*NDT1, indicated the presence of the typical MCF domain (PF00153, Pfam), in accordance with the InterPro and CDD servers. The main characteristic of the MCF domain is the occurrence of 3 tandem sequences (Repeats I – III) of approximately 100 amino acids residues with variations in their hydrophobicity; each one contains two α helix, with random coils connecting them. The domain consists of six α helices (H1 – H6) that spatially forms a channel with the central cavity open toward the outer face of the membrane and closed toward the inner face. The H1 – H6 α helices exhibit a transmembrane disposition and the N and *C terminus* are located in the outer face of the membrane, in agreement with the predicted topology from the CCTOP and PHYRE2 servers. Additionally, three short helices toward the inner membrane face (h12, h34 y h56) were identified; these are characteristic of the MCF (Figure 1A).

Multiple sequence alignments between *Lb*NDT1 and characterized NAD transporters from *A. thaliana* (NDT1 and NDT2) and *S. cerevisiae* (Ndt1p and Ndt2p), showed some additional characteristics of the MCF. The Px[DE]xx[KR] motif known as *mitochondrial energy transfer signature* (METS) was found toward the C-terminal region of each odd-numbered α helix (H1, H3 and H5), whose charged amino acids establish salt bridges (matrix network) which, in turn, maintain the central cavity closed. In an

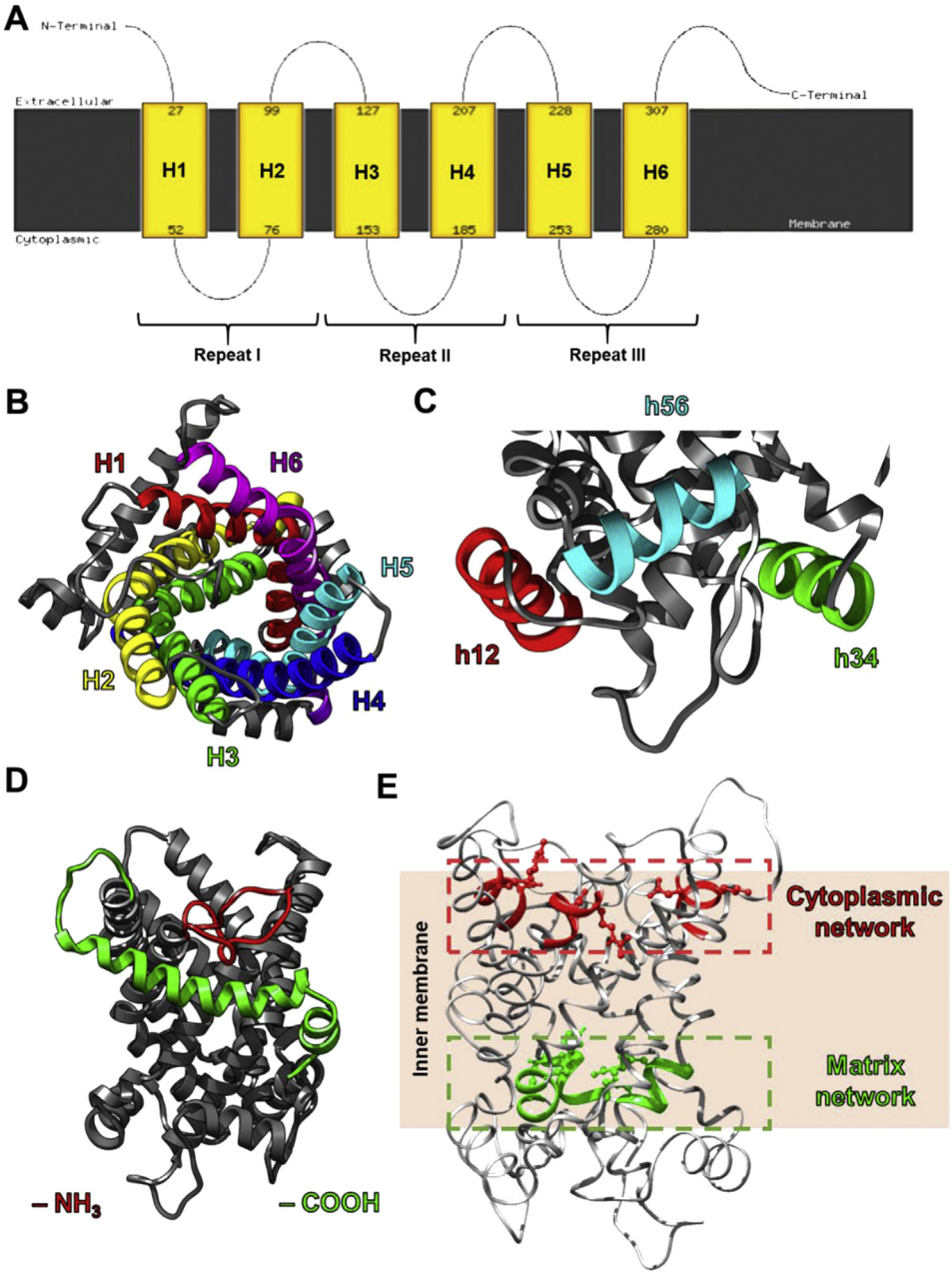

Figure 1. *Lb*NDT1 displays typical characteristics of the MCF. **A.** The topology model predicts the three tandem sequences (Repeats I–III) that establish six trans-membrane α helices (H1 – H6), and the N and C terminal regions toward the outer face of the membrane. **B-E.** A predictive model was obtained from the ROBETTA server, whose validation was completed by Ramachandran plots analysis with MolProbity. **B.** Top visualization of the six trans-membrane α helices (H1 – H6). **C.** Front visualization of the short α helices (h12, h34 and h56), located toward the inner face of the membrane. **D.** The N and C terminal regions are positioned towards the outer face of the membrane. **E.** Location of the Px[DE]xx[KR] (METS) (green) and [YF][DE]xx[KR] motifs (red). Images generated with UCSF Chimera (v 1.10.2).

analogous way, the [YF][DE]xx[KR] motif was identified toward the C-terminal region of the even-numbered α helices (H2, H4 and H6), whose charged residues also establish salt bridges (cytosolic network) that modulates the transport capacity. Furthermore, the predictive model of the *Lb*NDT1 candidate confirmed the spatial disposition of the six transmembrane α helices (H1–H6, Figure 1B) the three short helices toward the inner membrane face (h12, h34 y h56, Figure 1C), the N and C terminal regions toward the outer face of the membrane (Figure 1D), and the matrix and cytosolic networks (Figure 1E).

The *Lb*NDT1 predictive model was compared with the tertiary structure of the ADP/ATP transporter of *S. cerevisiae* ADT2 (PDB: 4C9G), which shows structural similarity with the *Lb*NDT1 candidate. The proteins share an identity of 24.02% and coverage of 88% in their primary structures, exhibiting the same conformation of the channel-like structure of the MCF domain, open at one end and closed at the opposite (Figure 2).

3.2. *LbNDT1 partially restores the phenotype of the S. cerevisiae mutant ΔNDT1 strain, deficient in mitochondrial NAD transport*

Functional assays of *Lb*NDT1 were carried out through complementation of the mutant yeast ΔNDT1, which is deficient in the mitochondrial transport of NAD. Thus, the *Lb*NDT1 open reading frame was amplified from gDNA by PCR; the amplicon was cloned in the pGEM-T Easy vector and sub-cloned into the pYES2 vector, appropriate for yeast expression. Both the mutant ΔNDT1 and the wild type strains were transfected with the recombinant vector pYES2/*Lb*NDT1, monitoring its growth in MS Ura$^-$ liquid medium supplemented with 2 % (w/v) raffinose or 2 %(v/v) ethanol (Figure 3). Initially, the usage of a fermentable carbon source such as raffinose in the medium does not cause a significant difference in the growth of each of the transfectants, although there is a difference with the untransfected mutant strain (ΔNDT1) (Figure 3A). When assessing growth with a non-fermentable source of carbon such as ethanol, attenuation of growth for each of the transfectants was evidence; nonetheless, this assay failed to make evident a difference in growth between the transfectant of the *Lb*NDT1 candidate and the negative control (empty pYES2) (Figure 3B), therefore the evaluation of growth on solid medium MS Ura$^-$ was conducted.

The evaluation of growth on MS Ura$^-$ solid medium was tested applying three serial dilutions of a yeast preparation in order to observe variations in growth rate by decreasing the number of cultured cells (Figure 3C). This assay indicated a notable difference in growth on both the pYES2/*Lb*NDT1 transfectant and the positive control (pYES2/*At*NDT2) relative to the negative control (empty pYES2) after 48 h (Day 2); however, this growth was lower in comparison with the wild type strain. This result demonstrates the ability of *Lb*NDT1 to partially restore the wild type phenotype of the *S. cerevisiae* mutant ΔNDT1 strain, confirming the functional identity of the *Lb*NDT1 protein.

3.3. *Endogenous LbNDT1 is expressed and located differentially in axenic amastigotes and promastigotes of L. braziliensis being N-glycosylated in both stages*

Immunodetection of the endogenous *Lb*NDT1 was carried out employing polyclonal avian antibodies (IgYs) produced in this study. The IgY's production involved the expression and purification of the recombinant thioredoxin tagged Trx-*Lb*NDT1 protein (theoretical MW 52.8 kDa) from the pBAD/*Lb*NDT1 vector, which was constructed by recombinant DNA technology. The expression of the recombinant Trx-*Lb*NDT1 protein was induced in *E. coli* BL21 (DE3) cells with L-Arabinose and monitored by SDS-PAGE. A prominent band with differential expression among the induced and non-induced cells was identified at the expected MW (Figure 4A) and detected with α–Trx antibodies by western blot (Figure 4B). The recombinant Trx-*Lb*NDT1 protein was purified from inclusion bodies (IB) and used as antigen for the production of avian α–*Lb*NDT1 antibodies, which specificity was determined by western blot (Figure 4C).

Once the specificity of the antibodies was tested, they were used for the immunodetection of endogenous *Lb*NDT1 on different protein extracts from axenic amastigotes and promastigotes of *L. braziliensis*. A

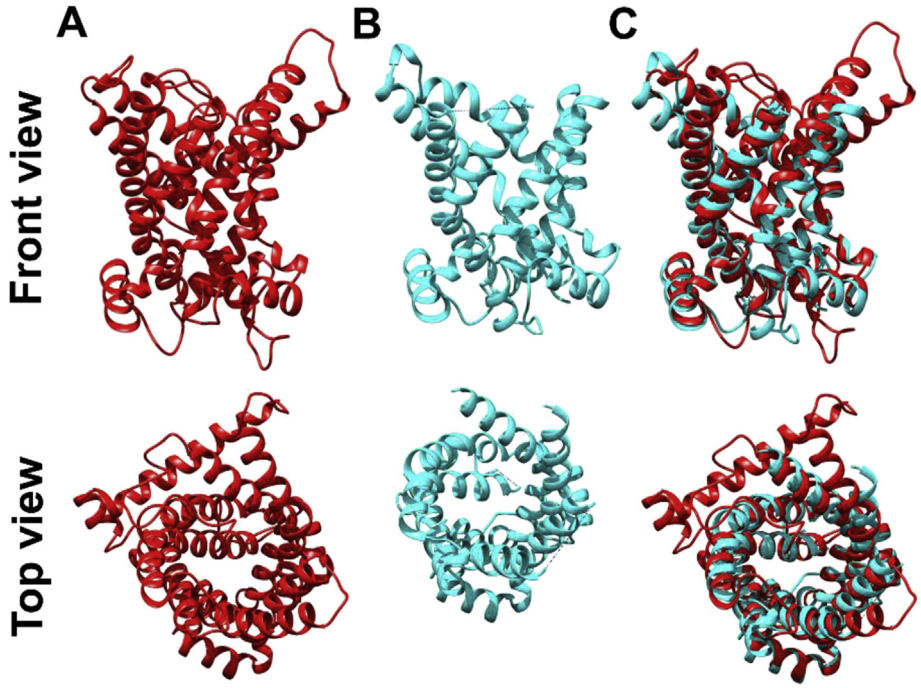

Figure 2. *Lb*NDT1 shows conformational similarity with MCF members. **A.** Predicted tertiary structure for *Lb*NDT1 (aa 1–362 red) by ROBETTA server. **B.** Tertiary structure of the ADP/ATP transporter of *S. cerevisiae* ADT2 (PDB 4C9G, cyan). **C.** Superposition between the *Lb*NDT1 model and the ADT2 tertiary structure (RMSD between 143 pairs of atoms: 1.090 Å). Images generated by UCSF-Chimera v 1.10.2.

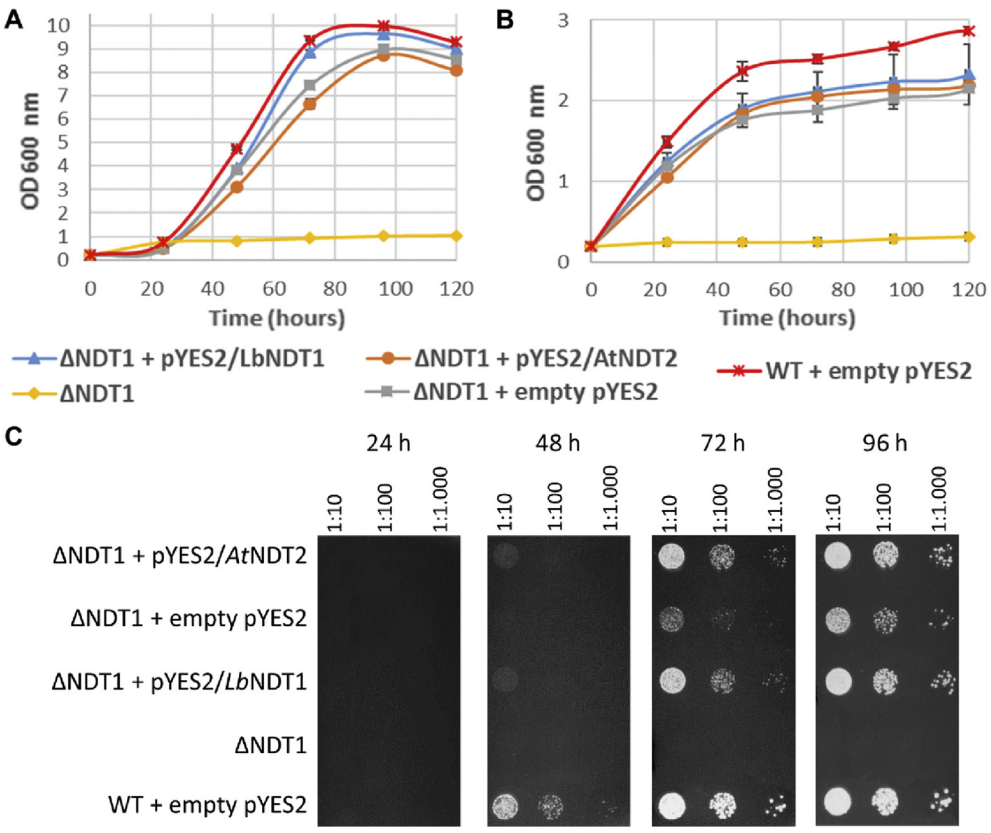

Figure 3. *Lb*NDT1 partially restores the phenotype of the *S. cerevisiae* mutant ΔNDT1 strain, deficient in mitochondrial NAD transport. Growth on MS Ura$^-$ medium was evaluated for transfectants ΔNDT1 + pYES2/*Lb*NDT1 (▲), ΔNDT1 + pYES2/*At*NDT2 (●), ΔNDT1 + empty pYES2 (■), untransfected ΔNDT1 (◆) and the wild strain + empty pYES2 (x). To monitor the growth in liquid medium, readings of OD_{600} were made every 24 h for 5 days. The solid medium images were documented for 4 days with the Imager® Gel DocTMXR image analyzer and the BIORAD™ Quantity One Basic 4.6.3 software. **A.** Growth in liquid medium containing a fermentable carbon source (raffinose 2% (w/v). **B.** Growth in liquid medium containing a non-fermentable carbon source (ethanol 2% (v/v) **C.** Growth in a solid medium containing a non-fermentable carbon source (ethanol 2% (v/v). Three biological replicates were performed for each assay.

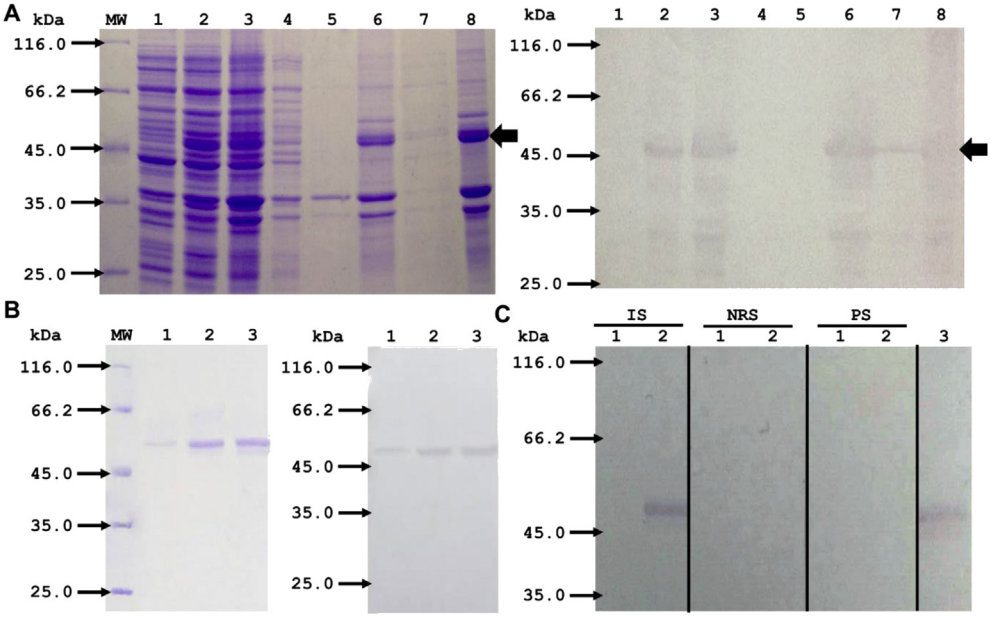

Figure 4. Production of polyclonal avian α–*Lb*NDT1 antibodies. **A.** Expression and purification of the recombinant Trx-*Lb*NDT1 protein from IB was monitored by SDS-PAGE, Coomassie R250 staining and western blot. Lanes: non-induced cells with pBAD202/*Lb*NDT1 (**1**) and induced (**2**). Insoluble fraction of induced cells (**3**). IB's washing with buffer I (**4**) and buffer II (**5**). Solubilized IB (**6**). Soluble (**7**) and insoluble (**8**) post dialysis fractions. **B.** Purification of the Trx-*Lb*NDT1 IB from preparative SDS-PAGE was monitored by SDS-PAGE, Coomassie R250 staining and western blot. Lanes: eluates from the upper (**1**), intermediate (**2**) and Lower (**3**) bands extracted from the preparative SDS-PAGE. **C.** The specificity of the immune α-*Lb*NDT1 (IS), non-related (NRS, from a different individual inoculated with 1X PBS as a control) and pre-immune sera (PS, from the same immunized individual before the inoculations as a control) at dilutions of 1:5000 was analyzed by western blot. Lanes: 300 ng of BSA (**1**) and recombinant Trx-*Lb*NDT1 protein (**2**). Commercial α-Trx antibody (1:6000) was used as a positive control (**3**). Membranes were developed with the alkaline phosphatase system. The right black arrows indicate the recombinant Trx-*Lb*NDT1 protein. MW, Thermo Scientific™ Pierce™ Unstained Protein Molecular Weight Marker (kDa).

specific 79.4 kDa band was detected in total and insoluble protein fractions in both parasite stages, as anticipated for a membrane protein due to its hydrophobicity (Figure 5A). The immunodetected band exhibited 40 kDa more than expected (39.8 kDa), probably corresponding to the *Lb*NDT1 protein modified by N-glycosylation, as reported for other transporters (Selcuk Unal et al., 2008). To prove this modification, a

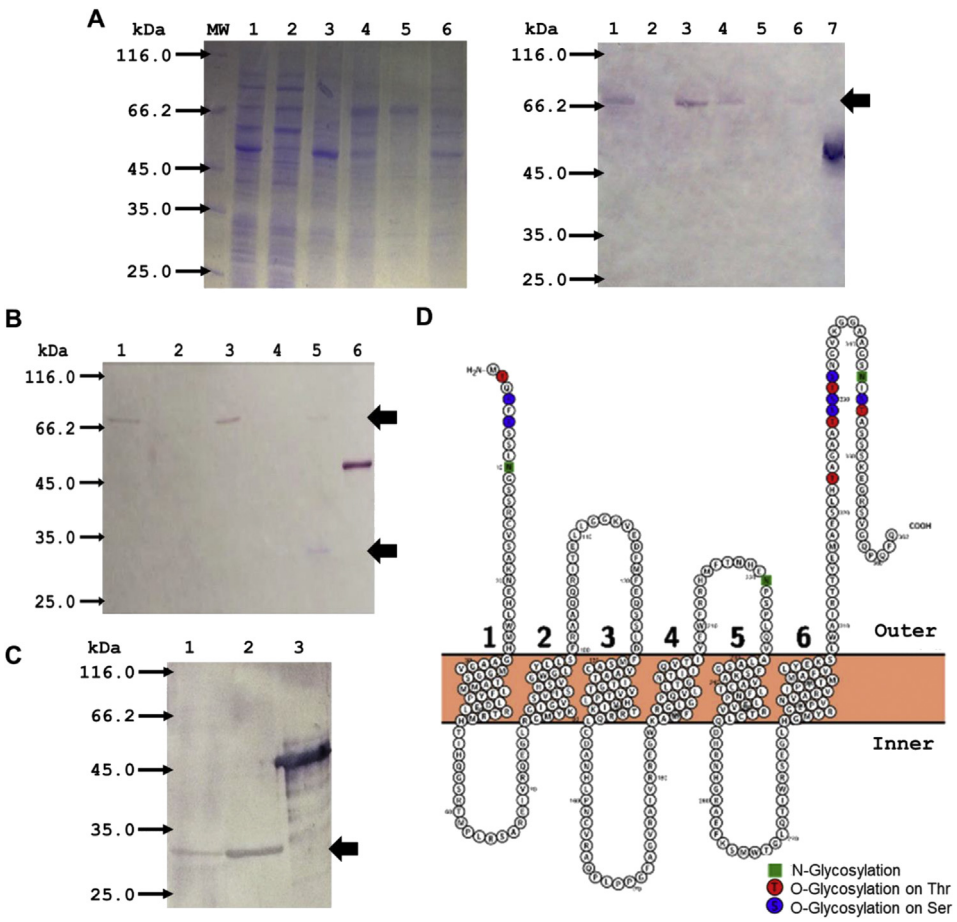

Figure 5. The endogenous N-Glycosylated *Lb*NDT1 was detected in insoluble protein fraction from axenic amastigotes and promastigotes of *L. braziliensis*. **A.** Detection of endogenous *Lb*NDT1 in promastigotes (lanes 1–3) and axenic amastigotes (lanes 4–6). SDS-PAGE and western blot: total proteins (**1**) & (**4**). Soluble (**2**) & (**5**) and insoluble protein fractions (**3**) & (**6**). Recombinant Trx-*Lb*NDT1 protein was loaded as a positive control (**7**). **B.** The de-glycosylation process of endogenous *Lb*NDT1 was follow by western blot. Total proteins (**1**). Soluble (**2**) and insoluble protein fractions (**3**). De-glycosylation of insoluble protein fraction by chemical treatment (**4**) or enzymatic treatment with PNGase F (**5**) Recombinant Trx-*Lb*NDT1 protein was loaded as a positive control (**6**). **C.** Immunodetection of the endogenous de-glycosylated *Lb*NDT1 (PNGase F treatment). Lanes: insoluble protein fraction of promastigotes (**1**) and axenic amastigotes (**2**). Recombinant Trx-*Lb*NDT1 protein was loaded as a positive control (**3**). Membranes were developed with the alkaline phosphatase system. The right arrows indicate the endogenous *Lb*NDT1 protein. **D.** Potential glycosylation sites for *Lb*NDT1 according its predicted topology. Each circle shows the amino acid sequence; green squares: N-Glycosilation on asparagine residues; red circles: O-Glycosylation on threonine and blue circles: O-Glycosylation on serine residues. Numbers 1–6 show the possible transmembrane regions.

non-denaturant enzymatic treatment with the PNGase F enzyme, specific for N-glycosylation, was done on the insoluble protein fraction of promastigotes of *L. braziliensis* and the recognition of *Lb*NDT1 on PNGase F-treated and -untreated samples with α-*Lb*NDT1 was performed by western blot (Figure 5B). Here, we could prove a partial de-glycosylation after the PNGase F treatment due to the detection of the 79.4 kDa band (glycosylated form) and a second specific 30 kDa band (10 kDa below the expected) corresponding to the endogenous *Lb*NDT1 without N-glycosylation in the PNGase F-treated sample. Considering these results, the recognition of the endogenous protein was performed on both parasite stages after de-glycosylation (Figure 5C) recognizing the 30 kDa band. The lower MW observed could be explained considering typical aberrant migration of membrane proteins in SDS-PAGE, as has been reported (Quiza et al., 1997; Rath et al., 2009). To identify potential glycosylation sites on the *Lb*NDT1, a bioinformatic approach using the GlycoEP, NetOGlyc-4.0 and NetNGlyc-1.0 servers was performed. These predictions revealed 3 potential sites for N-glycosylation and 11 for O-glycosylation at the N and C terminal regions of protein (Figure 5D).

Finally, the α–*Lb*NDT1 antibodies were used to analyze the subcellular location of the endogenous *Lb*NDT1 protein in both parasite stages through fluorescence microscopy (Figure 6). First, we checked the *in vitro* differentiation protocol and we could confirm the proper differentiation of promastigotes into amastigotes (Figure 6A). It was observed that in the promastigote stage, the *Lb*NDT1 protein is not localized in the kinetoplast, mitochondria or nucleus membranes; instead, a heterogeneous cytosolic localization was visualized. Interestingly, it was observed that in axenic amastigotes the endogenous *Lb*NDT1 protein exhibits a possible partial co-localization with mitochondria (Figure 6B).

4. Discussion

A unique cytosolic NMNAT, a key enzyme in the biosynthesis of NAD, has been identified in *L. braziliensis* (Contreras et al., 2015). Due to the requirements of this dinucleotide in the different subcellular compartments, it is critical to maintain adequate NAD levels within each of these. To achieve this requirement, a relationship between the NAD biosynthesis and transport systems has been established, as demonstrated in higher eukaryotic organisms, which have transporters that communicate subcellular compartments (Palmieri et al., 2009; Van Roermund et al., 2016; Todisco et al., 2006), as well as the expression of multiple NMNATs located in different organelles (Emanuelli et al., 1999, 2002; Hashida et al., 1999; Nikiforov et al., 2011). Similarly, in intracellular prokaryotic parasites, the absence of compartmentalization has led to the existence of a single NMNAT and the presence of multiple carriers in the cytoplasmic membrane (Haferkamp et al., 2004a, 2006), in order to preserve enough NAD levels within the cell. Accordingly, it is possible that intracellular organisms have eliminated redundant biosynthetic routes due to the plenty availability of nutrients from the host, favoring NAD transport.

To date no NAD transporters have been reported in protozoan parasites, however, the life traits of this kind of pathogens such as complex life cycles involving more than one host, extra and intracellular stages, probably promote the participation of this type of proteins to ensure infection, proliferation and survival processes. In this study, through a bioinformatic approach, a NAD transporter candidate was found in *L. braziliensis*. The *Lb*NDT1 candidate exhibits the main characteristics of the MCF (Figure 1), displaying the required structural elements to accomplish NAD transport through membranes. Likewise, the predictive

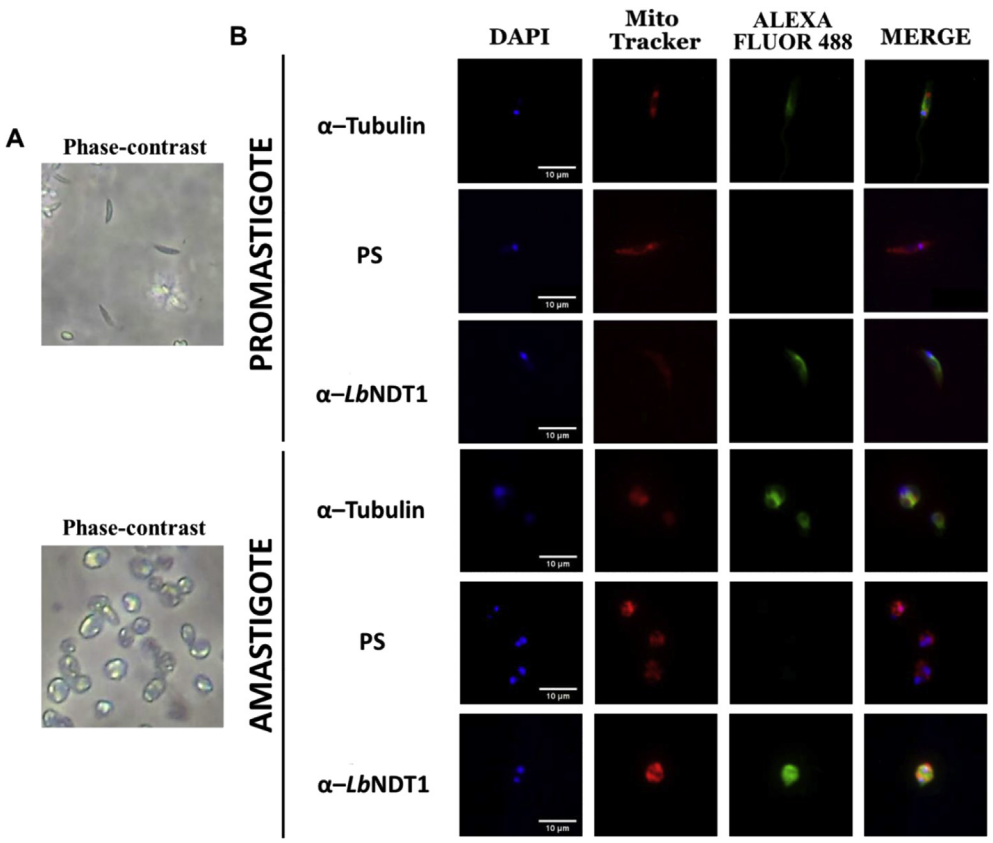

Figure 6. The endogenous *Lb*NDT1 protein exhibits a differential subcellular location in axenic amastigotes and promastigotes of *L. braziliensis*. **A.** *In vitro* differentiation process of promastigotes (Objective 20X) to axenic amastigotes (Objective 40X) observed under light microscope. **B.** The pre-immune (PI) and immune sera (α-*Lb*NDT1) were used in indirect immunofluorescence assay on fixed axenic amastigotes and promastigotes of *L. braziliensis*. Alexa Fluor 488: endogenous *Lb*NDT1 localization (green). MitoTracker: mitochondria localization (red). DAPI: nuclei localization (blue). Scale bars, 10 µm. Images were acquired with Nikon Eclipse C1 Plus microscope and the EZ-C1 Software. Objective 60X. *Lb*NDT1 and MitoTracker co-localization is evident in amastigotes.

model of the *Lb*NDT1 protein shows conformational similarity with resolved structures of the MCF members (Figure 2), allowing inferring its functionality.

Functional assay through complementation essays showed that *Lb*NDT1 protein has the ability to partially restore the growth rate of *S. cerevisiae* mutant ΔNDT1 strain in MS Ura^{-} medium supplemented with non-fermentable carbon sources such as ethanol (Figure 3). As previously reported (Todisco et al., 2006) this mutant has lower levels of mitochondrial NAD+ and NADH relative to the wild-type strain and hence a decreased activity of the NAD^{+}-dependent mitochondrial enzymes, pyruvate dehydrogenase (PDH) and acetaldehyde dehydrogenase (ACDH). Given that, ACDH catalyzes the limiting step in the metabolism of ethanol as a source of carbon in yeast, the ΔNDT1 mutant exhibits a growth delay; accordingly, partial restoration of the phenotype is due to the complementation of the deleted gene (Ndt1p) by an analogue with the same function, such as *Lb*NDT1 protein, which has the ability to transport NAD+. However, the flow of NAD+ provided by Ndtp2 is not discarded, as evidenced by the slight difference of ΔNDT1 growth relative to the wild type strain, compared to that of the double mutant ΔNDT1ΔNDT2 (Palmieri et al., 2009; Van Roermund et al., 2016; Todisco et al., 2006), despite this, the system of only one of the mutants was sufficient to prove the functionality of *Lb*NDT1 protein.

The endogenous *Lb*NDT1 protein was immunodetected in both parasite stages of *L. braziliensis* with our polyclonal α-*Lb*NDT1 avian antibodies, indicating that this transporter plays a crucial role in the cell cycle of the parasite. Taking into account that the parasite has a single cytosolic NMNAT, it is necessary the existence of NAD transport systems among different subcellular compartments, to preserver the NAD homeostasis. N-glycosylation of the endogenous *Lb*NDT1 protein was observed in both parasite stages, according to experimental evidence (Figure 5C) and computational predictions (Figure 5D). Glycosylation in trypanosomatids occurs in the lumen of the endoplasmic reticulum, where the core of carbohydrates, which varies among different species (Man(5, 6, 7, 9)GlcNAc2), is transferred from the dolichol-pyrophosphate-oligosaccharide (10–13 isoprene units) to an asparagine residue in the sequence Asn-X-Ser/Thr (X ≠ proline) of the protein to glycosylate, by paralogs of the STT3 catalytic subunit of the oligosaccharyltransferase (OST) complex present in mammals (Izquierdo et al., 2009; Stanley et al., 2009). Probably, *Lb*NDT1 glycosylation plays a role not only in the correct folding of the transporter, but also in the translocation towards the membrane of organelles such as the mitochondria and glycosome, allowing its correct functioning, as observed in mitochondrial glycoproteins Ydr065wp and Lpe10p of *S. cerevisiae* (Kung et al., 2009). Additionally, it was identified that the potential glycosylation sites are located at the N and C terminal regions, which makes these areas targets of possible regulation of the *Lb*NDT1 transport capacity.

The endogenous *Lb*NDT1 protein exhibits a MW of 30 kDa following the enzymatic treatment with the PNGase F enzyme, about 10 kDa below the predicted (39.8 kDa). This anomalous behavior in electrophoretic mobility is common to proteins with several transmembrane regions, as has been reported for other transporters, such as the human folate transporter PCFT (Selcuk Unal et al., 2008). This effect is produced by the high hydrophobicity of *Lb*NDT1 protein, leading to an incomplete denaturation, prevailing its native compact structure and therefore increasing migration when diminishing friction between the protein and the porous structure of the gel (El-Guindy et al., 2004). Conversely, glycosylation alters the protein local hydrophobicity and therefore the affinity with the SDS; as such, the electrophoretic mobility decreases due to the diminution of the net charge (Quiza et al., 1997; Selcuk Unal et al., 2008), explaining why the glycosylated form migrates approximately 40 kDa above the predicted weight (79.4 kDa).

A differential subcellular location for the endogenous *Lb*NDT1 protein was observed in both parasite stages of *L. braziliensis* (Figure 6). This is consistent with previous reports on the MCP6 transporter of *Trypanosoma brucei*, a member of the MCF for which its functionality has not yet been established; however, it was determined that, in the vector stage

(procyclic form), the transporter is predominantly located in the mitochondria, while in the bloodstream form, it is mainly located in the glycosome (Colasante et al., 2006). Regarding the *Lb*NDT1 protein, a possible partially mitochondrial localization was suggested in the intracellular form of the parasite (amastigote) and additional signals that may correspond to the transit of the protein through the endoplasmic reticulum and Golgi apparatus, where it is modified and trans-located to the mitochondria. At the functional level, there are significant differences in the mitochondrial bioenergetics of amastigotes compared with promastigotes (Mondal et al., 2014), for instance, amastigotes mainly depend on the tricarboxylic acids cycle (TCA) and mitochondrial respiration for energy obtaining rather than glycolysis (Dey et al., 2010). Considering that the main carbon source in this stage are amino acids, which are converted into TCA intermediates, wherein NAD+ is required for electron transfer and subsequent ATP synthesis by oxidative phosphorylation, the *Lb*NDT1 protein possibly plays the role of supplying NAD+ into the mitochondrial matrix for these processes to take place.

On the other hand, a heterogeneous cytosolic localization of the endogenous *Lb*NDT1 protein was observed in promastigotes, considering the differential location of the MCP6 transporter of *T. brucei*, it is possible that in *L. braziliensis*, the *Lb*NDT1 protein unveils a glycosomal location for the extracellular stage. In this stage the main carbon source is glucose and therefore its survival depends mainly on glycolysis (Subramanian et al., 2015) which takes place in the glycosome. Thus, it is conceivable that the *Lb*NDT1 protein transports the NAD required for glucose metabolism and ATP synthesis in this compartment (Michels et al., 2006). In turn, and as reported for other NAD carriers (Palmieri et al., 2009; Van Roermund et al., 2016; Todisco et al., 2006), it is possible that *Lb*NDT1 carries out a NAD+/ADP antiporter in the glycosome membrane during glycolysis. Additionally, it should be noted that the glycosome is a functionally very diverse organelle and, as such, this functionality varies depending on the cell cycle stage of the parasite. For example, since glycolysis is the main source of energy in promastigotes, the enzymes of this metabolic pathway will have a greater rate of translation compared to other pathways; on the contrary, in amastigotes, fatty acids are part of the main source of energy, thus the increased rate of translation will correspond to β-oxidation enzymes (Michels et al., 2006).

Finally, it is possible that NAD+ homeostasis in the different subcellular compartments is established by the other possible candidates found by bioinformatic tools but not included in this work, since it is known that members of the Mitochondrial Carrier Family have common substrates.

5. Conclusion

In this study a transporter of NAD (*Lb*NDT1) that shows the main characteristics of the Mitochondrial Carrier Family (MCF) was identified using bioinformatic and experimental tools. The *Lb*NDT1 transporter is expressed in axenic amastigotes and promastigotes of *L. braziliensis*, as evidenced by immunodetection assays; furthermore, it was proved that this is modified by N-Glycosylations in both parasite stages. Additionally, a possible partially mitochondrial localization for *Lb*NDT1 in axenic amastigotes and a possible glycosomal localization in promastigotes were proposed. Finally, the NAD transport capacity of *Lb*NDT1 was confirmed through complementation assays in *S. cerevisiae*. These results prove the existence of the first NAD transporter in protozoan parasites, the NDT1 of *L. braziliensis* (*Lb*NDT1).

Declarations

Author contribution statement

D. Herrera: Conceived and designed the experiments; Performed the experiments; Analyzed and interpreted the data; Wrote the paper.

L. Rodríguez: Performed the experiments; Wrote the paper.

C. Castellanos: Analyzed and interpreted the data.

M. Hernández: Conceived and designed the experiments; Performed the experiments; Analyzed and interpreted the data; Contributed reagents, materials, analysis tools or data; Wrote the paper.

Funding statement

This work was supported by Universidad Nacional de Colombia Sede Bogotá: Dirección de Investigación y Extensión (DIEB) (project number 37593) and Programa Jóvenes Investigadores (COLCIENCIAS) (call number 775–2017), Colombia.

Competing interest statement

The authors declare no conflict of interest.

Additional information

No additional information is available for this paper.

References

Agrimi, Gennaro, Russo, Annamaria, Scarcia, Pasquale, Palmieri, Ferdinando, 2012. The human gene SLC25A17 encodes a peroxisomal transporter of coenzyme A, FAD and NAD+. Biochem. J. 443 (1), 241–247.

Berger, Felicitas, Lau, Corinna, Dahlmann, Mathias, Ziegler, Mathias, 2005. Subcellular compartmentation and differential catalytic properties of the three human nicotinamide mononucleotide adenylyltransferase isoforms. J. Biol. Chem.

Blom, Nikolaj, et al., 2004. Prediction of post-translational glycosylation and phosphorylation of proteins from the amino acid sequence. Proteomics 4 (6), 1633–1649.

Chauhan, Jagat Singh, Rao, Alka, Raghava, Gajendra P.S., 2013. In silico platform for prediction of N-, O- and C-glycosites in eukaryotic protein sequences. PloS One 8 (6).

Colasante, Claudia, et al., 2006. Characterization and developmentally regulated localization of the mitochondrial carrier protein homologue MCP6 from *Trypanosoma brucei*. Eukaryot. Cell 5 (8), 1194–1205.

Contreras, Luis E., Neme, Rafik, Ramírez, María H., 2015. Identification and functional evaluation of *Leishmania braziliensis* nicotinamide mononucleotide adenylyltransferase. Protein Expr. Purif. 115, 26–33.

Dey, Ranadhir, et al., 2010. Characterization of a Leishmania stage-specific mitochondrial membrane protein that enhances the activity of cytochrome c oxidase and its role in virulence. Mol. Microbiol. 77 (2), 399–414.

Di Noia, Maria Antonietta, et al., 2014. The human SLC25A33 and SLC25A36 genes of solute carrier family 25 encode two mitochondrial pyrimidine nucleotide transporters. J. Biol. Chem. 289, 33137–33148.

Dobson, László, Reményi, István, Tusnády, Gábor E., 2015. CCTOP: a consensus constrained TOPology prediction web server". Nucleic Acids Res. 43, W408–W412.

El-Guindy, Ayman S., et al., 2004. N-linked glycosylation is required for optimal function of kaposi's sarcoma herpesvirus–encoded, but not cellular, interleukin 6. J. Exp. Med. 199 (4), 503–514.

Emanuelli, Monica, et al., 1999. Identication and characterization of YLR328W, the *Saccharomyces cerevisiae* structural gene encoding NMN adenylyltransferase. Expression and characterization of the recombinant enzyme. FEBS (Fed. Eur. Biochem. Soc.) Lett. 455, 13–17.

Emanuelli, Monica, et al., 2002. Identification and characterization of a second NMN adenylyltransferase gene in *Saccharomyces cerevisiae*. Protein Expr. Purif. 27, 357–364.

Fisher, Derek J., Fernández, Reinaldo E., Maurelli, Anthony T., 2013. *Chlamydia trachomatis* transports NAD via the Npt1 ATP/ADP translocase. J. Bacteriol. 195 (15), 3381–3386.

Forero-Baena, Nicolás, et al., 2015. Identification of a nicotinamide/nicotinate mononucleotide adenylyltransferase in *Giardia lamblia* (GlNMNAT). Biochim. Open 1, 61–69.

Gibbs, Richard A., 1990. DNA amplification by the polymerase chain reaction. Anal. Chem. 62, 1202–1214.

Haferkamp, Ilka, et al., 2004a. A candidate NAD transporter in an intracellular bacterial symbiont related to chlamydiae. Nature 432, 622–625.

Haferkamp, Ilka, et al., 2006. Tapping the nucleotide pool of the host: novel nucleotide carrier proteins of *Protochlamydia amoebophila*. Mol. Microbiol. 60 (6), 1534–1545.

Haferkamp, Ilka, Schmitz-esser, Stephan, Linka, Nicole, 2004b. A candidate NAD 1 transporter in an intracellular bacterial symbiont related to chlamydiae. Nature 432, 162–165.

Hashida, Shin-Nosuke, Takahashi, Hideyuki, Kawai-Yamada, Maki, Uchimiya, Hirofumi, 1999. *Arabidopsis thaliana* nicotinate/nicotinamide mononucleotide adenyltransferase (AtNMNAT) is required for pollen tube growth. FEBS (Fed. Eur. Biochem. Soc.) Lett. 455, 13–17.

Herrera, Edian A., et al., 2019. GlSir2.1 of *Giardia lamblia* is a NAD D-dependent cytoplasmic deacetylase. Heliyon 5 (4), e01520.

Izquierdo, Luis, et al., 2009. *Trypanosoma brucei* UDP-glucose:glycoprotein glucosyltransferase has unusual substrate specificity and protects the parasite from stress. Eukaryot. Cell 8 (2), 230–240.

Kato, Michiko, Lin, Su Ju, 2014. YCL047C/POF1 is a novel nicotinamide mononucleotide adenylyltransferase (NMNAT) in *Saccharomyces cerevisiae*. J. Biol. Chem. 289 (22), 15577–15587.

Kelley, Lawrence A., et al., 2015. The phyre2 web portal for protein modeling, prediction and analysis. Nat. Protoc. 10 (6), 845–858.

Kung, Li A., et al., 2009. Global analysis of the glycoproteome in *Saccharomyces cerevisiae* reveals new roles for protein glycosylation in eukaryotes. Mol. Syst. Biol. 5 (308).

Lagos M, Luisa F., Moran, Oscar, Camacho, Marcela, 2007. *Leishmania amazonensis*: anionic currents expressed in oocytes upon microinjection of MRNA from the parasite. Exp. Parasitol. 116 (2), 163–170.

Leprohon, Philippe, Légaré, Danielle, Ouellette, Marc, 2009. Intracellular localization of the ABCC proteins of Leishmania and their role in resistance to antimonials. Antimicrob. Agents Chemother. 53 (6), 2646–2649.

Lovell, Simon C., et al., 2003. Structure validation by C geometry: phi, psi and C-beta deviation. Proteins Struct. Funct. Genet. 50 (3), 437–450.

Michels, Paul A.M., Bringaud, Frédéric, Herman, Murielle, Hannaert, Véronique, 2006. Metabolic functions of glycosomes in trypanosomatids. Biochim. Biophys. Acta Mol. Cell Res. 1763 (12), 1463–1477.

Mitchell, Alex L., et al., 2019. InterPro in 2019: improving coverage, classification and access to protein sequence annotations. Nucleic Acids Res. 47 (D1), D351–D360.

Mondal, Subhasish, Roy, Jay Jyoti, Bera, Tanmoy, 2014. Characterization of mitochondrial bioenergetic functions between two forms of *Leishmania donovani* – a comparative analysis. J. Bioenerg. Biomembr. 46 (5), 395–402.

Moreno-González, Paula A., Diaz, Gonzalo J., Ramírez-Hernández, María H., 2013. Producción y purificación de Anticuerpos aviares (IgYs) a partir de Cuerpos de Inclusión de Una proteína recombinante central en el metabolismo del NAD. Rev. Colomb. Quím. 42 (2), 12–20. http://www.scielo.org.co/scielo.php?script=sci_arttext&pid=S0120-28042013000200002.

Nikiforov, Andrey, Dölle, Christian, Niere, Marc, Ziegler, Mathias, 2011. Pathways and subcellular compartmentation of NAD biosynthesis in human cells: from entry of extracellular precursors to mitochondrial NAD generation. J. Biol. Chem. 286 (24), 21767–21778.

Nikiforov, Andrey, Kulikova, Veronika, Ziegler, Mathias, 2015. The human NAD metabolome: functions, metabolism and compartmentalization. Crit. Rev. Biochem. Mol. Biol. 50 (4), 284–297.

Niño, Carlos H., et al., 2015. Identification of the nicotinamide mononucleotide adenylyltransferase of *Trypanosoma cruzi*. Mem. Inst. Oswaldo Cruz 110 (7), 890–897.

O'Hara, Jessica K., et al., 2014. Targeting NAD+ metabolism in the human malaria parasite *Plasmodium falciparum*. PloS One 9 (4), e94061.

Palmer, Ira, Wingfield, Paul T., 2012. Preparation and extraction of insoluble (Inclusion-Body) proteins from *Escherichia coli*. Curr. Protoc. Protein Sci. Chapter 6:Unit 6.3.

Palmieri, Ferdinando, et al., 2009. Molecular identification and functional characterization of *Arabidopsis thaliana* mitochondrial and chloroplastic NAD+ carrier proteins. J. Biol. Chem. 284 (45), 31249–31259.

Pettersen, Eric F., et al., 2004. UCSF Chimera - a visualization system for exploratory research and analysis. J. Comput. Chem. 25 (13), 1605–1612.

Quiza, Maribel, Dowton, Mark, Perry, Katie J., Sexton, Patrick M., 1997. Electrophoretic mobility and glycosylation characteristics of heterogeneously expressed calcitonin receptors. Endocrinology 138 (2), 530–539.

Rath, Arianna, et al., 2009. Detergent binding explains anomalous SDS-PAGE migration of membrane proteins. Proc. Natl. Acad. Sci. U. S. A. 106 (6), 1760–1765.

Roy, Suvra, Kumar, Vikash, 2014. A practical approach on SDS PAGE for separation of protein. Int. J. Sci. Res. 3 (8), 955–960.

Selcuk Unal, Ersin, Zhao, Rongbao, Qiu, Andong, Goldman, I. David, 2008. N-linked glycosylation and its impact on the electrophoretic mobility and function of the human proton-coupled folate transporter (HsPCFT). Biochim. Biophys. Acta Biomembr. 1778 (6), 1407–1414.

Smith, D.E., Fisher, P.A., 1984. Identification, developmental regulation, and response to heat shock of two antigenically related forms of a major nuclear envelope protein in Drosophila embryos: application of an improved method for affinity purification of antibodies using polypeptides immobilized on nitrocellulose blots. JCB (J. Cell Biol.) 99 (1 I), 20–28.

Stanley, P., Schachter, H., Taniguchi, N., 2009. N-Glycans. In: Varki, A., Cummings, R.D., Esko, J.D., et al. (Eds.), Essentials of Glycobiology, second ed. Cold Spring Harbor Laboratory Press, California: Cold Spring Harbor (NY). Chap. 8.

Steentoft, Catharina, et al., 2013. Precision mapping of the human O-GalNAc glycoproteome through SimpleCell technology. EMBO J. 32 (10), 1478–1488.

Subramanian, Abhishek, Jhawar, Jitesh, Sarkar, Ram Rup, 2015. Dissecting *Leishmania infantum* energy metabolism - a systems perspective. PloS One 10 (9), e0137976.

Sundar, Shyam, Singh, Bhawana, 2018. Emerging therapeutic targets for treatment of Leishmaniasis. Expert Opin. Ther. Targets 22 (6), 467–486.

Todisco, Simona, Agrimi, Gennaro, Castegna, Alessandra, Palmieri, Ferdinando, 2006. Identification of the mitochondrial NAD+ transporter in *Saccharomyces cerevisiae*. J. Biol. Chem. 281 (3), 1524–1531.

Van Roermund, Carlo W.T., et al., 2016. The peroxisomal NAD carrier from *Arabidopsis* imports NAD in exchange with AMP. Plant Physiol. 171 (3), 2127–2139.

VanLiden, Magali R., Hvidsten Skoge, Renate, Ziegler, Mathias, 2015. Discovery, metabolism and functions of NAD and NADP. Biochemist 37 (1), 9–13.

Yang, Ping-Chang, Mahmood, Tahrin, 2012. Western blot: technique, theory, and trouble shooting. N. Am. J. Med. Sci. 4 (9), 429.